Influence of Gait Cycle Normalization on Principal Activations

Gregorio Dotti
Department of Electronics and Telecommunications
Politecnico di Torino
Turin, Italy
gregorio.dotti@studenti.polito.it

Marco Ghislieri
Department of Electronics and Telecommunications
Politecnico di Torino
Turin, Italy
marco.ghislieri@polito.it

Samanta Rosati
Department of Electronics and Telecommunications
Politecnico di Torino
Turin, Italy
samanta.rosati@polito.it

Valentina Agostini
Department of Electronics and Telecommunications
Politecnico di Torino
Turin, Italy
valentina.agostini@polito.it

Marco Knaflitz
Department of Electronics and Telecommunications
Politecnico di Torino
Turin, Italy
marco.knaflitz@polito.it

Gabriella Balestra
Department of Electronics and Telecommunications
Politecnico di Torino
Turin, Italy
gabriella.balestra@polito.it

***Abstract*—The Clustering for Identification of Muscle Activation Pattern (CIMAP) algorithm has been recently proposed to cope with the high intra-subject variability of muscle activation patterns and to allow the extraction of principal activations (PAs), defined as those muscle activation intervals that are strictly necessary to perform a specific task. To assess differences between different PAs, gait cycle normalization techniques are needed to handle between- and within-subject variability. The aim of this contribution is to assess the effect of two different time-normalization techniques (Linear Length Normalization and Piecewise Linear Length Normalization) on PA extraction, in terms of inter-subject similarity. Results demonstrated no statistically significant differences in the inter-subject similarity between the two tested approaches, revealing, on the average, inter-subject similarity values higher than 0.64. Moreover, a statistically significant difference in the inter-subject similarity among muscles was assessed, revealing a higher similarity of PAs extracted considering the distal lower limb muscles. In conclusion, our results demonstrated that PAs extracted from healthy subjects during a walking task at comfortable walking speed are not affected by the time-normalization approach implemented.**

Keywords—EMG, gait analysis, locomotion, muscle activations, principal activations, time normalization.

I. Introduction

Gait analysis is commonly used to quantitatively assess normal and pathological functions of human walking [1], [2]. In particular, the study of muscle activation intervals extracted from surface electromyographic (sEMG) signals is especially important in clinical practice and research, as a valuable tool in the assessment of locomotion pathologies and rehabilitation protocols [3]. However, there is a great stride-to-stride variability in sEMG signals collected during gait [4], [5], even in healthy subjects. To cope with the high intra-subject variability of muscle activation patterns, Clustering for Identification of Muscle Activation Patterns (CIMAP) [6], [7] algorithm have been recently proposed and validated on several healthy and pathological sample populations [8]–[10].

The CIMAP algorithm is an agglomerative hierarchical clustering method that allows to group together the gait cycles showing similar sEMG onset-offset activation intervals [7]. Each cluster is described by an element (called prototype) that is calculated as the median value of all the sEMG activation intervals belonging to the same cluster. Then, Principal Activations (PAs) can be obtained as the intersection of all the cluster prototypes, describing the main activation pattern of a muscle during a gait analysis session. PAs represent those muscle activations that are *strictly necessary* to perform a task (e.g., walking) and describe the fundamental activation intervals of a specific muscle [9].

To assess differences between different muscle activation patterns, time-normalization techniques are needed to handle between- and within-subject variability due to slight changes of the walking speed [11]–[13] and stride-to-stride variability [4], [5]. Several methods have been proposed in literature to time-normalize gait cycles. Gait cycle data are either normalized by converting the time-samples to percentage of the gait cycle or by segmenting each gait cycle into subphases and time-normalizing each subphase.

In this contribution, we assessed the influence of these two different time-normalization approaches (Linear Length Normalization and Piecewise Linear Length Normalization approach) on PA extraction, in terms of PA inter-subject similarity.

II. Materials and Methods

A. Sample Population and Experimental Protocol

A sample population of 30 healthy subjects (gender: 15 females and 15 males, age: 27.8 ± 4.6 years, height: 172.8 ± 9.9 cm, weight: 68.2 ± 12.6 kg) was retrospectively analyzed considering gait data freely available in Zenodo repository (doi: 10.5281/zenodo.3932767) [14]. None of the enrolled volunteers reported lower limb injuries at the time of the experimental sessions or had neurological or musculoskeletal disorders that could affect gait performance.

All the enrolled volunteers underwent the same experimental protocol consisting of a walking task at a pre-selected speed. More specifically, the experimental protocol consisted of an overground walking at an average comfortable

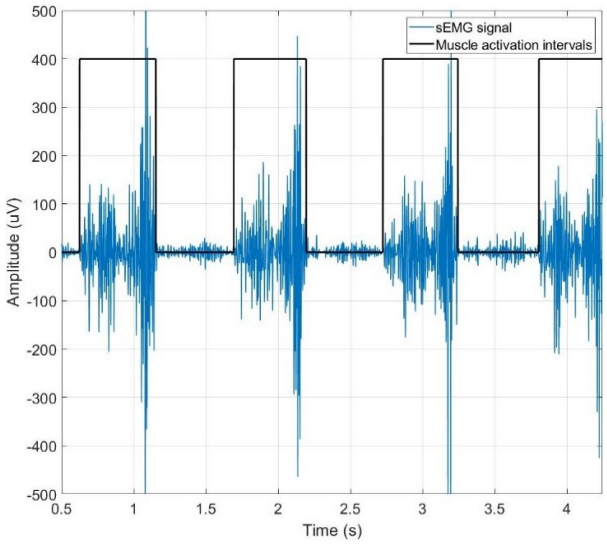

Figure 1. SEMG signal (blue line) acquired from the Tibialis Anterior (TA) muscle of a representative healthy subject of the sample population is represented along with the output of the muscle activity detector (black line). All the muscle activity shorter than 30 ms are rejected by means of the post-processing step.

walking speed of 1.4 m/s [15], [16] on an 18-m straight walkway, always starting with the same foot.

B. Data Acquisitions

During each experimental session, the following signals were simultaneously recorded [14]:

i. sEMG signals by means of a 16-channel wireless bipolar EMG system (Wave Plus wireless EMG, Cometa srl, Bareggio, Italy)
ii. Acceleration signals acquired through a tri-axial accelerometer (PicoEMG, Cometa srl, Bareggio, Italy)

SEMG probes were placed over the following 13 muscles of the dominant lower limb (right side): Gluteus Medius (GMD), Gluteus Maximus (GMA), Tensor Fasciae Latae (TFL), Rectus Femoris (RF), Vastus Medialis (VM), Vastus Lateralis (VL), Medial Hamstring (MH), Lateral Hamstring (LH), Tibialis Anterior (TA), Peroneus Longus (PL), Gastrocnemius Medialis (MGS), Gastrocnemius Lateralis (LGS), and Soleus (SOL).

Tri-axial accelerometer, instead, was placed over the second-last pair of shoe eyelets to obtain gait cycle timings (i.e., foot touchdown and lift-off time-instants) [17], [18].

SEMG signals were acquired with a sampling frequency of 2000 Hz, while acceleration signals with a sampling frequency of 142 Hz.

Gait data were then imported into MATLAB® release R2020b (The MathWorks Inc., Natick, MA, USA) to be processed offline by means of custom routines.

C. Data Processing

Before the application of the CIMAP algorithm, sEMG signals were pre-processed to extract muscle activation intervals and to time-segment gait cycles. Then, two different time-normalization approaches were applied to the pre-processed sEMG signals to assess the effect of different time-normalization approaches on principal activations (PAs).

1) Extraction of Muscle Activation Intervals

Firstly, sEMG signals were pass-band filtered through a 5th order Butterworth digital filter with a lower cut-off frequency of 40 Hz and an upper cut-off frequency of 300 Hz to remove motion and high-frequency artifacts [19].

Then, muscle activation onset/offset intervals were computed from the filtered sEMG signals, separately for the two tested time-normalization techniques, by means of a deep learning-based muscle activity detector. More specifically, the detector used in this study is based on Long Short-Term Memory (LSTM) neural networks [20], a widely used type of Recurrent Neural Networks (RNNs), specifically designed to recognized patterns and time-dependencies in sequential data, such as numerical time series, audio tracks, and texts [21].

Muscle activation intervals extracted through the muscle activity detector were defined as binary masks that were set equal to 1 in correspondence of a muscle activation and to 0 otherwise. Then, a post-processing step was applied to the detector's output to reject the erroneous transitions due to the stochastic nature of the sEMG signals. More specifically, muscle activation intervals shorter than 30 ms were discarded [22], [23].

Figure 1 shows an example of sEMG signal acquired from the Tibialis Anterior (TA) muscle of a representative healthy subject of the sample population with the indication of the muscle activation intervals computed through the deep learning-based detector.

2) Gait Cycle Segmentation and Time-Normalization

For each acquired muscle, the muscle activation intervals were time-segmented in gait cycles considering the touchdown and lift-off time-instants provided in the dataset [14].

Then, two different time-normalization approaches were tested to assess their influence on PAs: (*i*) the Linear Length Normalization (*LLN*) approach and (*ii*) the Piecewise Linear Length Normalization (*PLLN*) approach.

i. Linear Length Normalization (LLN): this approach linearly compresses/expands the time-axis of each gait cycle such that all gait cycles have the same number of samples [24]–[26]. More specifically, in this contribution, the gait cycle length is set equal to 1000 samples. According to the *LLN* approach, all the temporal differences between gait cycles due to changes in gait cycle duration are removed. However, even after the *LLN*, temporal differences between gait cycle sub-phases (i.e., stance and swing phase) may exist due to changes in gait speed [11]–[13], [27] or stride-to-stride variability [28].

ii. Piecewise Linear Length Normalization (PLLN): this approach firstly segments each gait cycle into epochs considering user-defined points of interest. Then, it piecewisely applies the *LLN* approach to time-normalize each gait cycle epoch [24], [29], [30]. The user-defined points of interest are usually determined based on kinematically relevant points within the gait cycle, such as foot touchdown and lift-off time-instants. In this study, each gait cycle was segmented in two different epochs, stance and swing, considering as points of interest the foot touchdown and lift-off time-instants provided in the dataset. Each gait cycle was then time-

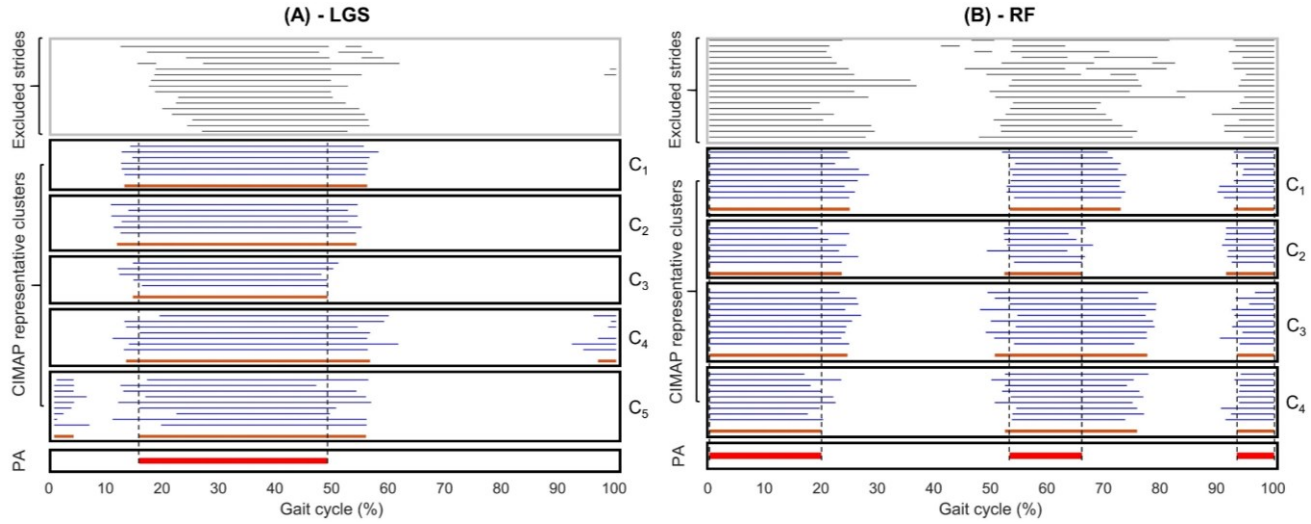

Figure 2. Example of application of the CIMAP algorithm to the (A) Lateral Gastrocnemius (LGS) and (B) Rectus Femoris (RF) muscles of a rapresentative healthy subject of the sample population. Blue lines inside each black rectangle (representative cluster) represent the time-normalized muscle activation intervals of the gait cycles that belong to the same representative cluster, while gray lines represent the excluded gait cycles. Orange lines represent the clusters' prototypes, defined as the median value of all the muscle activation intervals belonging to the same cluster. Red lines represent the Principal Activations (PAs), defined as the intersection of the representative clusters' prototypes.

normalized to 1000 time-samples, assigning 600 time-samples to the stance sub-phase and 400 time-samples to the swing sub-phase. The stance and swing durations were determined based on the foot-floor contact sequences usually adopted by healthy subjects during locomotion at comfortable walking speed [31], [32].

3) Extraction of Principal Activations (PAs) through CIMAP algorithm

The optimized version of the CIMAP algorithm [33] was applied on the normalized muscle activation intervals to extract PAs.

Figure 2 shows an example of application of the CIMAP algorithm to sEMG signals acquired from the Lateral Gastrocnemius (LGS) and Rectus Femoris (RF) muscles of a representative healthy subject of the sample population. Figure 2A and Figure 2B represent the time-normalized sEMG activation intervals (blue lines) grouped in clusters with the indication of the clusters' prototypes (orange lines) for the LGS and RF muscle, respectively.

Starting from a number of clusters equal to the number of analyzed gait cycles (each cluster contains only one gait cycle), the CIMAP algorithm iteratively merges the two "closest" clusters considering the Manhattan and Chebyshev distance metric, separately. The complete linkage method is used to assess the two "closest" clusters. According to the complete linkage method, the farthest distance between every pair of elements in the two considered clusters is considered as merging criterion. Two different dendrograms are then constructed: the first one considering the Manhattan distance and the second one considering the Chebyshev distance.

The final number of clusters (cutoff rule) for each dendrogram is selected to achieve:

i. Clusters characterized by a comparable and representative number of elements (C)

ii. Small intra-cluster variability (ICV), defined as the Euclidean distance between each element of the cluster and the corresponding cluster's prototype.

Since different numbers of final clusters may result from the two dendrograms, the best cutoff is automatically identified using an index that takes into account both the intra-cluster variability (ICV) and the number of elements within each cluster (N), as described in (1):

$$Cutoff = \frac{\sum_{i=1}^{n} ICV_i / n}{\sum_{i=1}^{n} |C_i|} \quad (1)$$

where n represents the number of clusters, $|C_i|$ is the number of gait cycles belonging to the i-th cluster, and ICV_i represents the intra-cluster variability of the i-th cluster

PAs are then extracted from the representative clusters (clusters that contains at least 10% of the total number of gait cycles) computing the intersection of the clusters' prototypes [33]. PAs are defined as 1000-samples binary masks that are set equal to 1 in correspondence of a principal muscle activation and to 0 otherwise.

Figure 2A and Figure 2B depict how the principal activations (red lines) are obtained from the significant clusters' prototypes for the LGS and RF muscle, respectively.

D. Inter-Subject Similarity of PAs

The influence of gait cycle normalization on PAs was studied in this contribution investigating the presence of changes in the inter-subject similarity of PAs. The Jaccard similarity index (J) [22],[23] was used to compute similarity between couples of PAs as defined in (2).

$$J_{i,j} = \frac{PA_i \cap PA_j}{PA_i \cup PA_j} \quad (2)$$

where PA_i and PA_j represent the principal activations extracted from the i-th and j-th subject, respectively. The Jaccard similarity index (J) ranges between 0 (i.e., complete dissimilarity) and 1 (i.e., complete similarity).

The average J_k value was computed over all the possible couples of PAs extracted from the k-muscle, while the grand-average of the J_k indexes ($\bar{J}$) was computed over all the k-muscles.

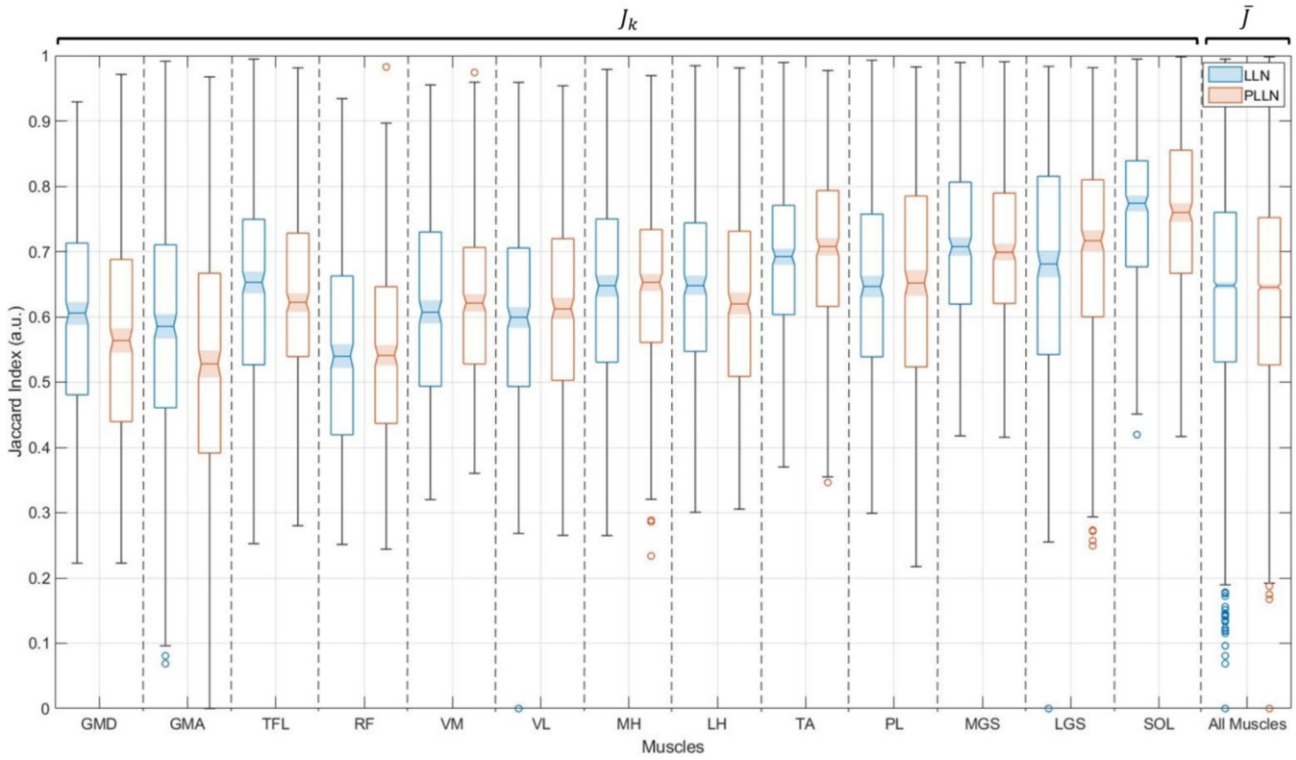

Figure 3. Boxplots of the average J_k values and grand-average $\bar{J}$ values computed considering the *LLN* (blue) and *PLLN* (red) approaches. Outliers are indicated by circles.

The MATLAB® function "*jaccard*" was used to compute the Jaccard similarity indexes.

E. Statistical Analysis

Two-way analysis of variance (ANOVA) followed by a *post-hoc* analysis with Tukey's adjustment for multiple comparisons was used to test the differences in the Jaccard similarity indexes between Approach (*LLN* and *PLLN*) and Muscles. The significance level (α) was set equal to 0.05. The statistical analysis was performed using the Statistical and Machine Learning Toolbox of MATLAB®.

III. Results

The subjects walked at an average speed of 1.4 m/s ± 0.1 m/s. On the average, a dataset of 63 ± 11 gait cycles was assessed for each subject. In terms of stance and swing durations, an average value of 63.6% ± 0.03% and 36.4% ± 0.03% was found considering the stance and the swing phase, respectively.

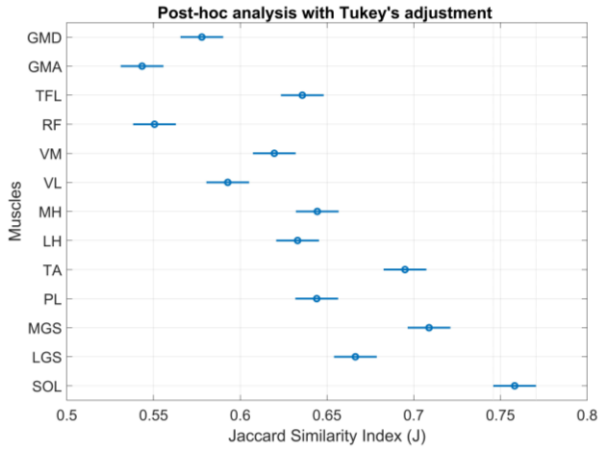

Figure 4. Results of the *post-hoc* analysis with Tukey's adjustment for multiple comparisons. Blue circles represent the average Jaccard similarity indexes (J_k), while blue intervals represent the corresponding standard errors for each *k*-muscle.

An average $\bar{J}$ index of 0.64 ± 0.17 and 0.63 ± 0.17 was found considering the *LLN* and *PLLN* approach, respectively. Two-way ANOVA showed no statistically significant differences in Jaccard similarity indexes between Approach (p = 0.843), while statistically significant differences were detected between Muscles ($p < 0.0001$).

Figure 3 shows the boxplots of the Jaccard similarity indexes (J_k) relative to each of the 13 acquired muscles and the boxplot of the grand-average over all the muscles ($\bar{J}$).

Figure 4, instead, represents the results of the *post-hoc* analysis with Tukey's adjustment for multiple comparisons.

IV. Discussion and Conclusion

In this contribution, we assessed the effect of two different sEMG time-normalization approaches on principal activation extraction in terms of inter-subject similarity of PAs. More specifically, among all the time-normalization approaches published in literature, the Linear Length Normalization (*LLN*) and the Piecewise Linear Length Normalization (*PLLN*) were tested.

No statistically significant differences in the inter-subject similarity values between *LLN* (0.64 ± 0.17) and *PLLN* (0.63 ± 0.17) approach, while statistically significant differences were detected between inter-subject similarity values extracted from different muscles. In particular, the muscles of the leg (i.e., SOL, LGS, MGS, PL, and TA) revealed higher values of Jaccard similarity indexes with respect to the shank muscles (i.e., GMD, GMA, TFL, RF, VM, VL, MH, and LH). Results revealed that PAs are, overall, more similar across

subjects considering distal lower limb muscles, suggesting a higher repeatability of the propulsive (PL, MGS, LGS, and SOL) and foot clearance control functions (TA) with respect to the biomechanical functions of the proximal lower limb muscles.

In conclusion, our results demonstrated that PAs extracted from healthy subjects during a walking task at comfortable walking speed are not affected by the time-normalization approach implemented. Further studies are necessary to test the effect of different gait cycle normalization approaches also on sEMG data acquired at different walking speeds.

REFERENCES

[1] F. Di Nardo, A. Mengarelli, E. Maranesi, L. Burattini, and S. Fioretti, "Gender differences in the myoelectric activity of lower limb muscles in young healthy subjects during walking," *Biomed. Signal Process. Control*, vol. 19, pp. 14–22, 2015, doi: 10.1016/j.bspc.2015.03.006.

[2] A. Mengarelli, E. Maranesi, L. Burattini, S. Fioretti, and F. Di Nardo, "Co-contraction activity of ankle muscles during walking: A gender comparison," *Biomed. Signal Process. Control*, vol. 33, pp. 1–9, 2017, doi: 10.1016/j.bspc.2016.11.010.

[3] V. Agostini, M. Ghislieri, S. Rosati, G. Balestra, and M. Knaflitz, "Surface Electromyography Applied to Gait Analysis: How to Improve Its Impact in Clinics?," *Front. Neurol.*, vol. 11, pp. 1–13, 2020, doi: 10.3389/fneur.2020.00994.

[4] V. Agostini, A. Nascimbeni, A. Gaffuri, P. Imazio, M. G. Benedetti, and M. Knaflitz, "Normative EMG activation patterns of school-age children during gait," *Gait Posture*, vol. 32, no. 3, pp. 285–289, 2010, doi: https://doi.org/10.1016/j.gaitpost.2010.06.024.

[5] F. Di Nardo, A. Mengarelli, G. Ghetti, and S. Fioretti, "Statistical analysis of EMG signal acquired from tibialis anterior during gait," in *IFMBE Proceedings*, 2014, vol. 41, pp. 619–622, doi: 10.1007/978-3-319-00846-2_153.

[6] S. Rosati, V. Agostini, M. Knaflitz, and G. Balestra, "Muscle activation patterns during gait: A hierarchical clustering analysis," *Biomed. Signal Process. Control*, vol. 31, pp. 463–469, 2017, doi: 10.1016/j.bspc.2016.09.017.

[7] S. Rosati, C. Castagneri, V. Agostini, M. Knaflitz, and G. Balestra, "Muscle contractions in cyclic movements: Optimization of CIMAP algorithm," 2017, doi: 10.1109/EMBC.2017.8036762.

[8] V. Agostini, S. Rosati, C. Castagneri, G. Balestra, and M. Knaflitz, "Clustering analysis of EMG cyclic patterns: A validation study across multiple locomotion pathologies," in *2017 IEEE International Instrumentation and Measurement Technology Conference (I2MTC)*, May 2017, pp. 1–5, doi: 10.1109/I2MTC.2017.7969746.

[9] C. Castagneri, V. Agostini, S. Rosati, G. Balestra, and M. Knaflitz, "Longitudinal assessment of muscle function after Total Hip Arthroplasty : Use of clustering to extract principal activations from EMG signals," in *2018 IEEE International Symposium on Medical Measurements and Applications (MeMeA)*, 2018, pp. 1–5, doi: 10.1109/MeMeA.2018.8438802.

[10] C. Castagneri, V. Agostini, S. Rosati, G. Balestra, and M. Knaflitz, "Asymmetry Index in Muscle Activations," *IEEE Trans. Neural Syst. Rehabil. Eng.*, vol. 27, no. 4, pp. 772–779, 2019, doi: 10.1109/TNSRE.2019.2903687.

[11] M. H. Schwartz, A. Rozumalski, and J. P. Trost, "The effect of walking speed on the gait of typically developing children," vol. 41, pp. 1639–1650, 2008, doi: 10.1016/j.jbiomech.2008.03.015.

[12] C. Kirtley, M. W. Whittle, and R. J. Jefferson, "Influence of walking speed on gait parameters," *J. Biomed. Eng.*, vol. 7, no. 4, pp. 282–288, 1985, doi: 10.1016/0141-5425(85)90055-X.

[13] M. J. Chung and M. J. J. Wang, "The change of gait parameters during walking at different percentage of preferred walking speed for healthy adults aged 20-60 years," *Gait Posture*, vol. 31, no. 1, pp. 131–135, 2010, doi: 10.1016/j.gaitpost.2009.09.013.

[14] I. Mileti *et al.*, "Muscle activation patterns are more constrained and regular in treadmill than in overground human locomotion," *Front. Bioeng. Biotechnol.*, vol. 8, no. October, 2020, doi: 10.3389/fbioe.2020.581619.

[15] A. Santuz, A. Ekizos, L. Janshen, V. Baltzopoulos, and A. Arampatzis, "On the Methodological Implications of Extracting Muscle Synergies from Human Locomotion," *Int. J. Neural Syst.*, vol. 27, no. 5, 2017, doi: 10.1142/S0129065717500071.

[16] A. Santuz, A. Ekizos, and A. Arampatzis, "A Pressure Plate-Based Method for the Automatic Assessment of Foot Strike Patterns During Running," *Ann. Biomed. Eng.*, vol. 44, no. 5, pp. 1646–1655, 2016, doi: 10.1007/s10439-015-1484-3.

[17] A. Santuz, A. Ekizos, N. Eckardt, A. Kibele, and A. Arampatzis, "Challenging human locomotion: Stability and modular organisation in unsteady conditions," *Sci. Rep.*, vol. 8, no. 1, pp. 1–13, 2018, doi: 10.1038/s41598-018-21018-4.

[18] A. Santuz *et al.*, "Neuromotor Dynamics of Human Locomotion in Challenging Settings," *iScience*, vol. 23, no. 1, 2020, doi: 10.1016/j.isci.2019.100796.

[19] C. J. De Luca, L. Donald Gilmore, M. Kuznetsov, and S. H. Roy, "Filtering the surface EMG signal: Movement artifact and baseline noise contamination," *J. Biomech.*, vol. 43, no. 8, pp. 1573–1579, 2010, doi: 10.1016/j.jbiomech.2010.01.027.

[20] S. Hochreiter and J. Schmidhuber, "Long Short-Term Memory," *Neural Comput.*, vol. 9, no. 8, pp. 1735–1780, Nov. 1997, doi: 10.1162/neco.1997.9.8.1735.

[21] A. Graves, "Generating Sequences With Recurrent Neural Networks," pp. 1–43, 2013, [Online]. Available: http://arxiv.org/abs/1308.0850.

[22] R. a Bogey, L. a Barnes, and J. Perry, "Computer algorithms to characterize individual subject EMG profiles during gait.," *Arch. Phys. Med. Rehabil.*, vol. 73, no. 9, pp. 835–841, 1992, doi: 0003-9993(92)90155-P [pii].

[23] P. Bonato, T. D'Alessio, and M. Knaflitz, "A statistical method for the measurement of muscle activation intervals from surface myoelectric signal during gait," *IEEE Trans. Biomed. Eng.*, 1998, doi: 10.1109/10.661154.

[24] N. E. Helwig, S. Hong, E. T. Hsiao-Wecksler, and J. D. Polk, "Methods to temporally align gait cycle data," *J. Biomech.*, vol. 44, no. 3, pp. 561–566, 2011, doi: 10.1016/j.jbiomech.2010.09.015.

[25] D. A. Winter, *The Biomechanics and Motor Control of Human Gait*. Waterloo, Ontario, Canada: University of Waterloo Press, 1987.

[26] J. Perry, "Gait Analysis: Normal and Pathological Function," *J. Pediatr. Orthop.*, vol. 12, p. 815, 1992, doi: 10.1001.

[27] B. W. Stansfield, S. J. Hillman, M. E. Hazlewood, and J. E. Robb, "Regression analysis of gait parameters with speed in normal children walking at self-selected speeds," *Gait Posture*, vol. 23, no. 3, pp. 288–294, 2006, doi: 10.1016/j.gaitpost.2005.03.005.

[28] F. Di Nardo *et al.*, "A new parameter for quantifying the variability of surface electromyographic signals during gait: The occurrence frequency," *J. Electromyogr. Kinesiol.*, vol. 36, pp. 25–33, 2017, doi: 10.1016/j.jelekin.2017.06.006.

[29] H. Sadeghi, P. Allard, F. Prince, and H. Labelle, "Symmetry and limb dominance in able-bodied gait: A review," *Gait Posture*, vol. 12, no. 1, pp. 34–45, 2000, doi: 10.1016/S0966-6362(00)00070-9.

[30] H. Sadeghi, P. A. Mathieu, S. Sadeghi, and H. Labelle, "Continuous curve registration as an intertrial gait variability reduction technique," *IEEE Trans. Neural Syst. Rehabil. Eng.*, vol. 11, no. 1, pp. 24–30, 2003, doi: 10.1109/TNSRE.2003.810428.

[31] V. Agostini, G. Balestra, and M. Knaflitz, "Segmentation and classification of gait cycles," *IEEE Trans. Neural Syst. Rehabil. Eng.*, vol. 22, no. 5, pp. 946–952, 2014, doi: 10.1109/TNSRE.2013.2291907.

[32] M. G. Benedetti, V. Agostini, M. Knaflitz, V. Gasparroni, M. Boschi, and R. Piperno, "Self-reported gait unsteadiness in mildly impaired neurological patients: an objective assessment through statistical gait analysis.," *J. Neuroeng. Rehabil.*, vol. 9, p. 64, 2012, doi: 10.1186/1743-0003-9-64.

[33] S. Rosati, C. Castagneri, V. Agostini, M. Knaflitz, and G. Balestra, "Muscle contractions in cyclic movements: Optimization of CIMAP algorithm," *Proc. Annu. Int. Conf. IEEE Eng. Med. Biol. Soc. EMBS*, pp. 58–61, 2017, doi: 10.1109/EMBC.2017.8036762.

[34] P. Jaccard, "the Distribution of the Flora in the Alpine Zone.," *New Phytol.*, vol. 11, no. 2, pp. 37–50, 1912, doi: 10.1111/j.1469-8137.1912.tb05611.x.

[35] J. M. Vargas, "The Probabilistic Basis of Jaccard's Index of Similarity," *Artic. Syst. Biol.*, 1996, doi: 10.1093/sysbio/45.3.380.